J. Wind Eng. Ind. Aerodyn. 156 (2016) 62–71

Contents lists available at ScienceDirect

Journal of Wind Engineering and Industrial Aerodynamics

journal homepage: www.elsevier.com/locate/jweia

Vulnerability assessment for the hazards of crosswinds when vehicles cross a bridge deck

Se-Jin Kim, Chul-Hwan Yoo, Ho-Kyung Kim *

Dept. of Civil and Environmental Engineering, Seoul National University, 1 Gwanak-ro, Gwanak-gu, Seoul 151-744, South Korea

ARTICLE INFO

Article history:
Received 1 February 2016
Received in revised form
20 June 2016
Accepted 14 July 2016
Available online 28 July 2016

ABSTRACT

A new procedure to assess the crosswind hazard of operating a vehicle over a bridge deck has been developed using a probabilistic approach that utilizes long-term wind data at bridge sites as well as the aerodynamic properties of bridge decks and vehicles. The proposed procedure for safety assessment considers the probabilities of two accident types: sideslip and overturning. The vulnerability of vehicles to crosswinds is represented by the number of days for traffic control that would be required to secure vehicle safety over a period of one year. The distribution of wind speed over a bridge deck was estimated from a section model wind tunnel test. A sea-crossing bridge was selected as an example, and a series of case studies were performed to identify the influential factors affecting vehicle vulnerability to crosswinds: vehicle type and loaded weight, the position of a running vehicle over a bridge deck, the bridge alignment relative to the dominant wind direction, and vehicle speed.

1. Introduction

Strong gusts of wind can reduce vehicle safety when crossing a wind-exposed structure such as a bridge. As the number of long-span bridges increases throughout the world, this issue increases in importance, and many wind-induced vehicle accidents have been reported in past decades (Baker and Reynolds, 1992; Zhu et al., 2012). In order to prevent these accidents, the installation of windscreens or traffic-control actions have been proposed for protecting vehicles from high-speed winds. These measures can effectively mitigate the vulnerability of vehicle safety while crossing a bridge under a crosswind. However, excessive designs for windscreens or overly complicated traffic control guidelines can result in a negative effect in terms of aerodynamic stability and excessive cost/benefit ratios. Hence, a vulnerability assessment that adequately considers the surrounding environmental or structural shapes of bridges is necessary.

Extensive studies for the simulation of vehicle movements and an evaluation of wind-induced accident risks for given conditions have been conducted. Baker (1986, 1987, 1991a, 1991b, 1991c) constructed an analytical framework that can be used to evaluate aerodynamic forces and vehicle motion. He performed several wind tunnel tests to examine the aerodynamic forces that act on vehicles according to wind direction, and introduced a simplified safety analysis method. Xu and Guo (2003) and Chen and Cai (2004) also presented a framework for computer simulation that considers wind-bridge-vehicle interactions. They performed time-domain analysis to evaluate vehicle motion and estimated accident-causing wind speeds for various vehicle speeds. Similarly, Batista and Perkovič (2014) proposed a simple static analysis method to estimate critical perpendicular wind speeds.

In order to propose guidelines for the decision-making process with respect to the need for windscreens, Kwon et al. (2011) and Kim et al. (2011) presented a method for assessing the frequency of exposure to hazardous crosswinds. They estimated the expected days for vehicle accidents through stochastic analysis using long-term wind data, and estimated the total expected cost induced by accidents. Using this method, decisions for the construction of windscreens can be justified from an economic perspective. However, the method focused on overall assessment strategy, rather than considering details such as the positions of running vehicles over a bridge deck. Therefore, it is necessary to use wind details and structural conditions to develop a vulnerability assessment method for the operation of vehicles over a bridge deck that is exposed to frequent lateral winds.

This study proposes a new assessment procedure for evaluating the crosswind hazards of a bridge by implementing a section-model wind-tunnel testing and a probabilistic long-term wind analysis at a particular bridge site by considering four affecting factors: 1) vehicle type, 2) loading lane, 3) bridge direction, and 4) vehicle speed. As a measure of the vulnerability of vehicles to crosswind hazards, a frequency of traffic control that will secure vehicle safety criteria is proposed. The proposed procedure was

* Corresponding author.
E-mail addresses: sejin09@snu.ac.kr (S.-J. Kim), jahad1010@snu.ac.kr (C.-H. Yoo), hokyungk@snu.ac.kr (H.-K. Kim).

http://dx.doi.org/10.1016/j.jweia.2016.07.005

applied to an example bridge and a series of parameter studies were conducted to estimate the factors governing the vulnerability of vehicles to crosswind hazards.

2. Proposed assessment procedure

A probabilistic procedure is proposed for the assessment of vehicle safety in crosswind. The basic concept involves the use of the critical wind speeds for a target vehicle and long-term wind data measured at a particular bridge site. The final output from this procedure is the number of days needed for traffic control, N_C, which is the expected number of days per year that the maximum wind speed will exceed the critical wind level. Using N_C as a risk index, the vulnerability of a bridge for vehicle safety can be evaluated. This index provides intuitive information on the degree of vehicle safety.

The proposed procedure consists of three steps: (1) estimation of a cumulative distribution function for wind data, (2) estimation of critical wind speed, and, (3) estimation of the number of days for traffic control (N_C). The procedure is illustrated in Fig. 1. With this procedure, the critical wind speeds of vehicles and the cumulative distribution functions of wind data are estimated for 16 directions. This is done to consider the variations in the critical wind speed of a vehicle according to wind direction. In fact, the most vulnerable wind direction generally is not 90° because the vehicle is also subject to its own speed. Therefore, considering all wind directions is desirable for a reasonable assessment.

Also, a wind tunnel test is performed to evaluate the effect of bridge girders on the wind speed over the deck. Undisturbed oncoming wind speeds and the wind speeds over traffic lanes are different due to the flow interruption by bluff girders, and the ratio between these two wind speeds must be considered. This ratio is referred to as the wind speed modification factor, and it is measured via wind tunnel testing. Further details of each step are introduced in the following sections.

2.1. Step 1. estimating the cumulative distribution function of wind data

The aim of step 1 is to estimate the cumulative distribution function for 16 directions with consideration paid to the effect that girders would exert on wind speed. The probability distribution can be estimated by using a specific probability distribution model. In the present study, the wind data provided from weather stations is in the form of the daily maximum value, and, therefore, a Generalized Extreme Value (GEV) distribution model is used. This probability model combines three typical extreme value distribution models: Gumbel, Fréchet and Weibull distributions. The equation for the cumulative distribution function for a GEV distribution model is expressed as follows.

$$F(X < x;\, \mu,\, \sigma,\, \xi) = \exp\left\{ -\left[1 + \xi \frac{x - \mu}{\sigma} \right]^{-1/\xi} \right\} \tag{1}$$

where σ is the scale parameter, μ is the location parameter, and ξ is the shape parameter. These three parameters can be estimated for 16 wind directions by applying the maximum likelihood estimation (Coles, 2001).

Prior to estimating the parameters, wind speed data should be modified using a correction factor and wind speed modification factors in order to consider the differences in wind speeds between a weather station and traffic lanes.

First, a correction factor is calculated, which is the ratio between wind speeds at a weather station and at a bridge site with consideration given to the differences in terrain roughness and elevation. Korean Society of Civil Engineers (2006) proposes a correction factor as follows:

$$\begin{aligned} C &= \left(\frac{z_{G1}}{z_1} \right)^{\alpha 1} \cdot \left(\frac{z_2}{z_{G2}} \right)^{\alpha 2}, \qquad z_2 \geq z_b \\ &= \left(\frac{z_{G1}}{z_1} \right)^{\alpha 1} \cdot \left(\frac{z_b}{z_{G2}} \right)^{\alpha 2}, \qquad z_2 < z_b \end{aligned} \tag{2}$$

where subscript 1 refers to the weather station and subscript 2 refers to the bridge site; α is the exponent that governs the shape of the wind profile; z is the height of the measurement point; z_G is the gradient height of the wind profile, and z_b is the minimum height.

In addition, we can estimate the wind speed modification factor, R_v, which refers to the ratio of the mean wind speed, V, at a certain location over a bridge deck to that of the undisturbed oncoming wind speed, V_∞, as shown in Eq. (3) and Fig. 2. With this

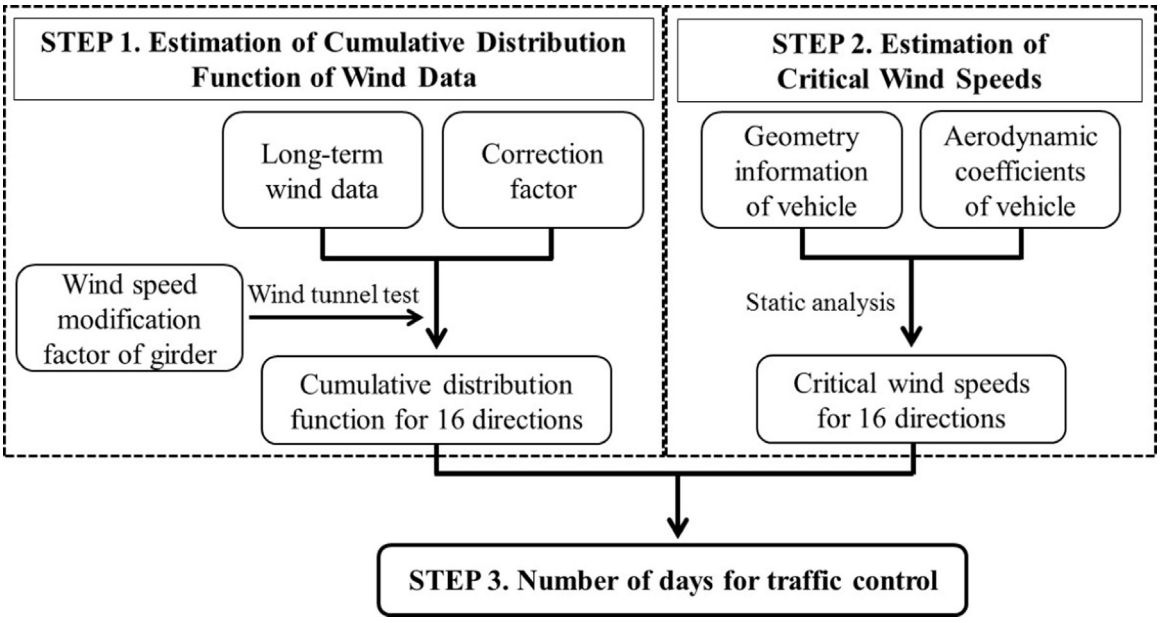

Fig. 1. Diagram of assessment procedure.

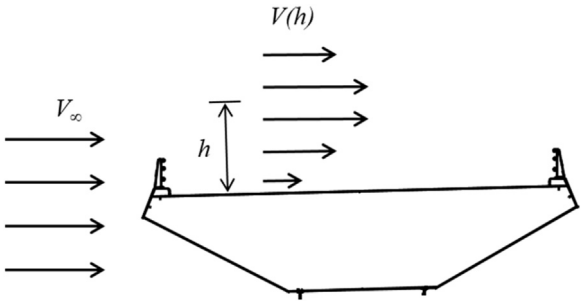

Fig. 2. Undisturbed wind speed, V_∞, and wind speed profile, V, over the deck.

wind speed data, the interruption effect that the girders have on the wind flow can be considered.

$$R_v = \frac{V}{V_\infty} \tag{3}$$

Normally, the modification factor changes along the height over the deck because the girders and guardrails disturb the wind flow. Therefore, a wind tunnel test is performed to estimate this variation.

2.2. Step 2. estimation of critical wind speed

In order to calculate the critical wind speed, a researcher must define the criteria that will be used to judge whether a vehicle is in a risky situation. The criteria can be defined by the types of accidents that might occur. For this study, sideslip and overturning accident types were considered, and these are shown in Fig. 3. The critical wind speed for each accident type implies the minimal wind speed, which satisfies the following criteria for each case.

- Sideslip: the side friction force of one of the vehicle axles reaches its maximum static friction force.
- Overturning: one of the contact forces of a wheel becomes zero.

In order to calculate reaction forces such as a contact force and a side friction force, simple static analysis introduced by Batista and Perkovič (2014) was adopted. They derived equations for reaction forces from equilibrium, constraint and constitutive equations, as follows.

$$\begin{aligned}
F_{z1} &= \frac{1}{2}\frac{b(mg-F_L)}{a+b} - \frac{1}{2}\frac{hF_S+M_R}{c} - \frac{1}{2}\frac{hF_D+M_P}{a+b}\\
F_{z2} &= \frac{1}{2}\frac{a(mg-F_L)}{a+b} - \frac{1}{2}\frac{hF_S+M_R}{c} + \frac{1}{2}\frac{hF_D+M_P}{a+b}\\
F_{z3} &= \frac{1}{2}\frac{b(mg-F_L)}{a+b} + \frac{1}{2}\frac{hF_S+M_R}{c} - \frac{1}{2}\frac{hF_D+M_P}{a+b}\\
F_{z4} &= \frac{1}{2}\frac{a(mg-F_L)}{a+b} + \frac{1}{2}\frac{hF_S+M_R}{c} + \frac{1}{2}\frac{hF_D+M_P}{a+b}
\end{aligned} \tag{4}$$

where a and b are the distance of the front and rear axles from the center of gravity, respectively; c is the track width; h is the vertical distance between the ground and the center of gravity; g is the acceleration of gravity; m is the vehicle mass; F_{zj} (j=1, 2, 3, 4) are the vertical contact forces; F_D, F_S, and F_L are the drag force, the side force, and the lift force that collectively make up the aerodynamic forces. M_R, M_P, and M_Y are the rolling moment, the pitching moment and the yawing moment, which are the aerodynamic moments.

The equations that were used to calculate the side friction forces acting on each axis are as follows (Batista and Perkovič, 2014):

$$\begin{aligned}
F_{y,front} &= F_{y1}+F_{y3} = \frac{bF_S+M_Y}{a+b} - \left(\frac{i_1+i_2}{2}q - f_R\right)\frac{hF_S+M_R}{a+b}\\
F_{y,rear} &= F_{y2}+F_{y4} = \frac{aF_S-M_Y}{a+b} + \left(\frac{i_1+i_2}{2}q - f_R\right)\frac{hF_S+M_R}{a+b}
\end{aligned} \tag{5}$$

where $F_{y,front}$ and $F_{y,rear}$ are the side friction forces acting on the front and rear axles, respectively; i_1 and i_2 are the variables which only can be 0 or 1 according to whether the axle is driven or not for front and rear axles. If i_1 or i_2 are 1, this means that the corresponding axle is driven. f_R is the rolling resistance coefficient which is assumed to be constant; q is the traction parameter which is the ratio between traction force and vertical reaction force. Equation to estimate q is as follows (Batista and Perkovič, 2014):

$$q = \frac{(a+b)\left[F_D + f_R(mg-F_L)\right]}{(i_1 b + i_2 a)(mg-F_L) + (i_2-i_1)(hF_D+M_P)} \tag{6}$$

Since Eqs. (4)–(6) are derived from static analysis, it is noteworthy that suspension or inertia effect were not taken into account. This shortage can be effectively overcome in further study by adopting such a quasi-static theory (Baker, 2015), in which the suspension, cant, and road curvature effects were considered.

Aerodynamic forces and moments acting on a vehicle can be expressed in terms of the wind speed and direction. Unless the vehicle stops, an apparent wind speed and effective wind direction, which is the wind speed and direction that the vehicle actually experiences, should be obtained by vector summation of the vehicle speed and the true wind speed. When the vehicle speed is $\boldsymbol{v}$, the speed of the true wind is $\boldsymbol{w}$ and the wind direction is β, the apparent wind speed, $\boldsymbol{V}$, and effective wind direction, ψ, can be estimated as follows based on Fig. 4.

$$|\mathbf{V}|^2 = \left(|\mathbf{v}| + |\mathbf{w}|\cos\beta\right)^2 + |\mathbf{w}|^2\sin^2\beta \tag{7}$$

$$\psi = \arctan\frac{|\mathbf{w}|\sin\beta}{|\mathbf{v}| + |\mathbf{w}|\cos\beta} \tag{8}$$

With calculated apparent wind speed, $\boldsymbol{V}$, and effective wind direction, ψ, the aerodynamic forces and moments acting on a

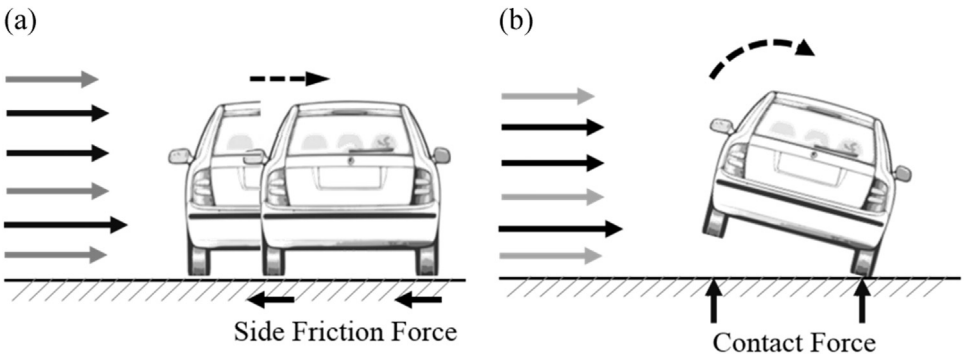

Fig. 3. Considered accident types. (a) Sideslip accident and (b) Overturning accident.

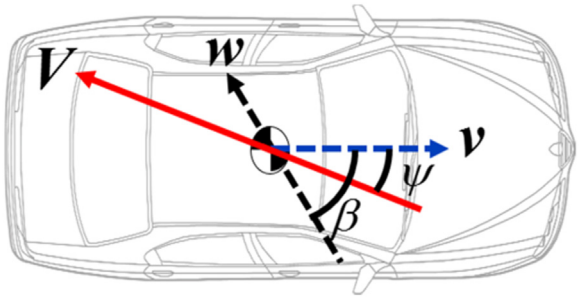

Fig. 4. Three wind vectors: vehicle speed ***v***, true wind speed ***w***, and apparent wind speed ***V***.

vehicle can be estimated as follows.

$$F_D = C_D A\frac{\rho V^2}{2} \quad F_s = C_s A\frac{\rho V^2}{2} \quad F_L = C_L A\frac{\rho V^2}{2} \tag{9}$$

$$M_R = C_R Ah\frac{\rho V^2}{2} \quad M_P = C_P Ah\frac{\rho V^2}{2} \quad M_Y = C_Y Ah\frac{\rho V^2}{2} \tag{10}$$

where C_D, C_S, C_L, C_R, C_P, and C_Y are the aerodynamic coefficients of a vehicle for drag force, side force, lift force, rolling moment, pitching moment, and yawing moment, respectively. ρ is the air density ($=1.2245$ kg/m^3) and A is the frontal area of the vehicle. Aerodynamic coefficients are functions of the effective wind direction, ψ.

2.3. Step 3. estimating the number of Days needed for traffic control

The probability that the actual wind speed will exceed a critical level, P_E, was evaluated by considering 16 wind directions, as follows.

$$P_E = \sum_{\text{all direction}} P_i \times P_{E|dir=i} \tag{11}$$

where P_i is the probability that the direction of the wind is i and $P_{E|dir=i}$ is the conditional probability that a daily maximum wind speed will exceed the critical wind speed for i. P_i can be obtained from the frequency analysis of wind data.

In order to compute $P_{E|dir=i}$, the critical wind speed and cumulative probability function for i are required. $P_{E|dir=i}$ refers to the probability that critical wind speeds will be exceeded, as shown in Fig. 5. Since the estimated critical wind speeds are defined for sideslip and overturning, as shown in Fig. 5, the larger value should be $P_{E|dir=i}$, as follows.

$$P_{E|dir=i} = \max\left(P_{E|dir=i,sideslip}, P_{E|dir=i,overturning}\right) \tag{12}$$

Once the P_E is determined, the annual expected number of days for traffic control, N_C, can be calculated by multiplying P_E by 365 days, as follows.

$$N_C = 365 \times P_E \tag{13}$$

3. Application to a bridge

The proposed method was applied to a cable-stayed bridge with twin steel deck girders, as shown in Fig. 6. The deck provides a total of 6 traffic lanes and 2 emergency lanes. The width and depth of the deck is 41 m and 4 m, respectively. The bridge crosses an open sea, and the deck is located 32 m above the water surface.

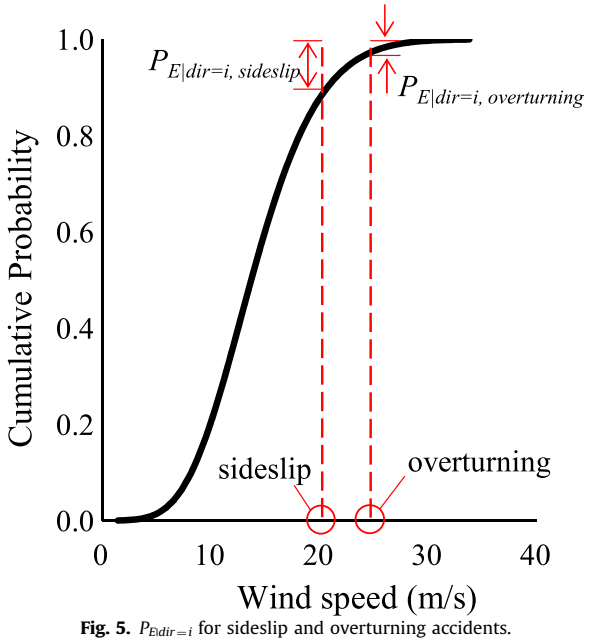

Fig. 5. $P_{E|dir=i}$ for sideslip and overturning accidents.

3.1. Wind data and wind characteristics of the bridge site

The wind data were obtained from a nearby weather station: 10 min. averaged wind speeds for 30 years from 1979 to 2009. The data were reported in daily maximum values and all data were classified into 16 wind directions. The total number of daily maximum wind data measurements used for the estimation was 10,550. The anemometer at the weather station was located 10 m above the ground.

The correction factor used to convert the wind data from the weather station to that of the bridge site was estimated as $C=1.38$ from Eq. (2) by applying the exponents, α, of the weather station and the bridge site, 0.16 and 0.12, respectively, and the gradient heights, z_G, of the two sites, which were 600 m and 500 m, respectively (Korean Society of Civil Engineers, 2006).

The weather station monitored the wind data in 16 wind directions at an interval of 22.5°. Fig. 7 shows a wind rose diagram for the 10 min. averaged daily maximum wind speed data corrected to the bridge site. The percentage of frequencies for each direction are shown in Table 1. According to Fig. 7 and Table 1, NW and NNW were the dominant wind directions that were perpendicular to the longitudinal direction of the bridge. These frequencies correspond to P_i in Eq. (11).

3.2. Wind tunnel test

A wind tunnel test was performed at the Boundary Layer Wind Tunnel at Hyundai E&C to estimate the effect of the girders on wind speed. The width of the test section was 4.5 m, the height was 2.5 m, and the length was 30.0 m.

A section model of the deck was prepared to a scale of 1/50; the height was 0.079 m; the length was 2.4 m; and, the width was 0.82 m. Fig. 8 shows the shape of the section model of the bridge. In order to estimate the wind speed profile across traffic lanes, the wind speeds were observed at five locations for each traffic lane at heights of 1, 2, 2.5, 3, and 4 m in a prototype scale, according to the height of a normal truck. The heights of the measuring points were equivalent to 2, 4, 5, 6, and 8 cm, respectively, in the scale model. Wind speed profiles for each traffic lane were measured via a hotwire anemometer at a wind speed of 8 m/s.

Fig. 9 shows the profiles of modification factors across the windward and leeward lanes. The profiles for windward lanes show rapid changes in the wind speed along the height over the

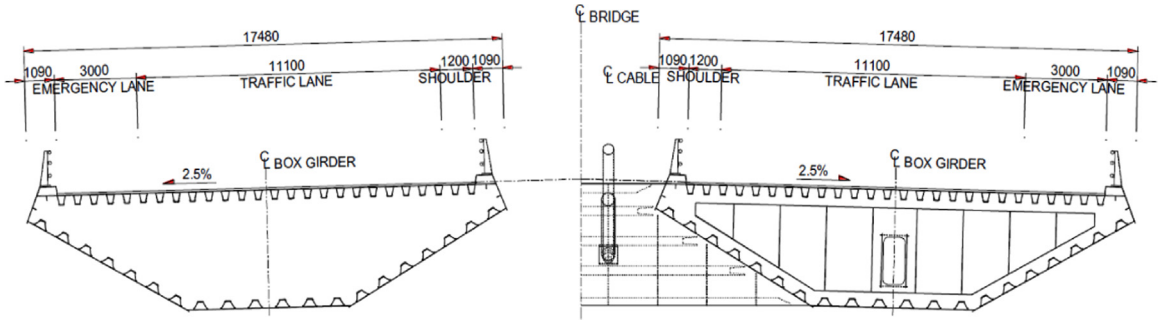

Fig. 6. Cross-section of a deck (unit: mm).

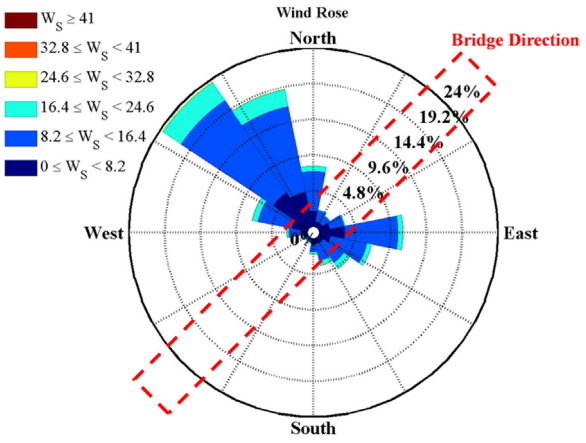

Fig. 7. Wind rose at the bridge site.

Table 1
Frequencies for each wind direction.

Direction	Frequency (%)	Direction	Frequency (%)
N	8.2	S	2.1
NNE	2.3	SSW	0.6
NE	1.9	SW	0.5
ENE	3.5	WSW	0.7
E	11.3	W	2.8
ESE	7.2	WNW	7.6
SE	5.1	**NW**	**23.6**
SSE	3.8	**NNW**	**18.9**

deck. An acceleration of the wind speed was also observed above a height of 3 m. The differences in the profiles for windward and leeward lanes seemed to originate from the gap between the two box girders as well as from the guardrail on the windward side. The rapid change in the wind profile along the height could result in a large rolling moment for vehicles.

Before applying the above results to modifications in the wind speed data, representative modification factors were determined for each traffic lane. Representative modification factors were determined by adopting the concept of a wind speed profile that would be equivalent to the height and to the effect of the side force and rolling moment for vehicles.

Two processes were necessary, as shown in Fig. 10. The first process involved simplifying the wind speed profile to a step function based on the measuring points. By this simplifying process, a more conservative wind profile was obtained, which meant an increase in the total integrated area of the profile. In the second process, an equivalent wind speed was estimated by transforming the simplified profile to a uniform profile. This transformation was performed in order to secure the magnitude of the aerodynamic forces acting on a vehicle. Since the wind load per unit area is proportional to the square of the wind speed, the square of the wind speed profile had to be integrated. For the side forces that cause sideslip, Eq. (14) transforms the wind speed profile to an equivalent uniform profile

$$U_{eq} = \sqrt{(1/4m)\int_0^{4m} u^2(z)dz} \tag{14}$$

where u is the wind speed at z-meter above the deck, and U_{eq} denotes the equivalent wind speed. By applying this equation, the modification factors from lane 1 to 6 were obtained as 0.86, 0.77, 0.74, 0.78, 0.81, and 0.82, respectively. For the rolling moment that causes overturning, Eq. (15) was used to transform the wind speed profile to an equivalent uniform profile, and to estimate the modification factors for each lane: 1.05, 0.95, 0.91, 0.91, 0.93, and 0.93, respectively.

$$U_{eq} = \sqrt{(2/(4m)^2)\int_0^{4m} u^2(z)zdz} \tag{15}$$

By multiplying the wind speed data from a deck location by these modification factors, the wind speed over the deck could be estimated. The modification factor varies according to the type of accident as well as the running lane of a vehicle. For the examined bridge, the modification factors for an overturning accident were larger than those for sideslip. Also, the wind speeds over the outside lanes were greater than those over the inside lanes.

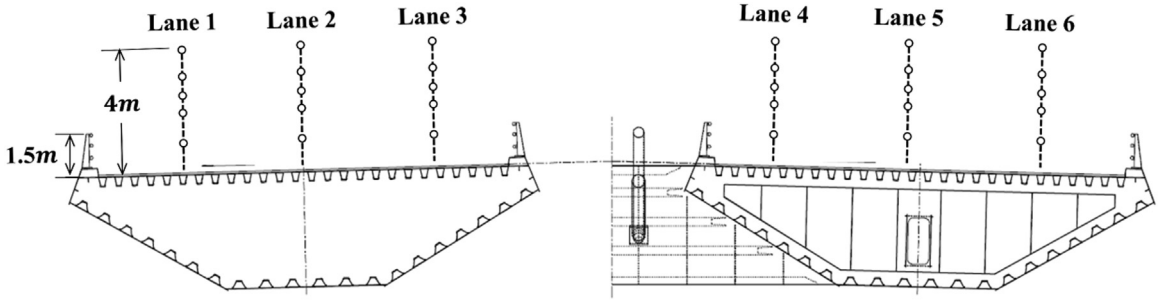

Fig. 8. Measuring points of wind speed over each traffic lane.

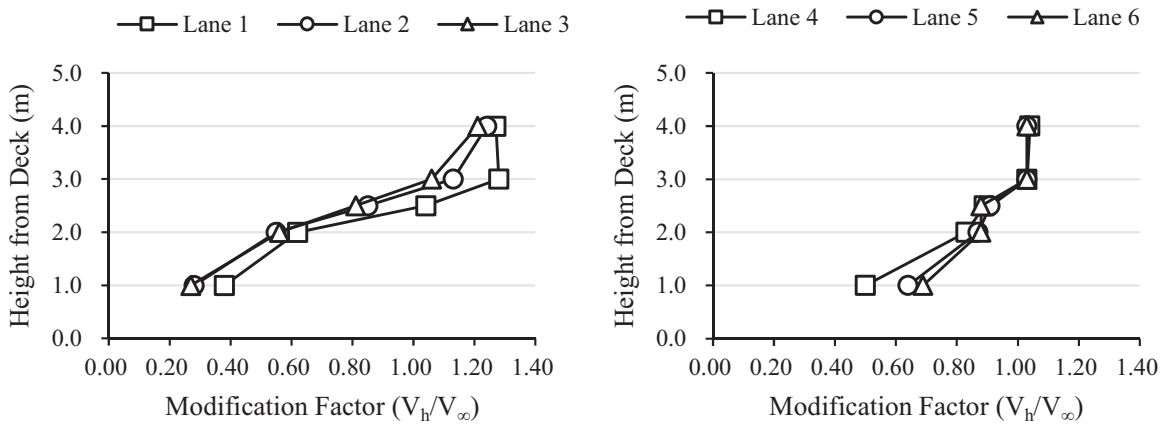

Fig. 9. Profiles of modification factors.

3.3. Cumulative distribution function according to wind direction

The cumulative distribution functions were estimated for each wind direction and for each traffic lane by utilizing the wind speed modification factors and terrain roughness correction factor. Three parameters of the GEV distribution were obtained for one data set corresponding to each specific combination of wind direction and traffic lane. A total of 192 data sets provided the same number of cumulative distribution functions for all wind directions and traffic lanes. With the estimated parameters, we were able to calculate $P_{El dir=i}$.

Fig. 11 lists the estimated cumulative distribution function and estimated parameters for one selected case in the NW direction, the first lane, and a sideslip accident. The estimated cumulative distribution function shows a high degree of goodness-of-fit with the observed data. The same levels were observed for the other 15 wind directions.

3.4. Critical wind speed according to wind direction

Five vehicle models were investigated: a passenger car, a coach, a large van, a tractor-trailer, and a truck. The dimensions and aerodynamic coefficients of the vehicles were estimated and proposed by Baker (1987) and Batista and Perkovič (2014). Aerodynamic coefficients were defined for effective wind directions ranging from 0 ° to 180 °. Fig. 12 and Table 2 show the dimensions of the investigated vehicles. The aerodynamic coefficients of a coach, as an example, are plotted in Fig. 13, based on the definition proposed by Baker (1987).

The critical wind speeds for all wind directions can be estimated for sideslip and overturning. The vehicle speed was assumed to be 50 km/h, which can be regarded as a speed limit for a sedan and a van during high-wind conditions (Kwon and Jeong, 2005). Fig. 14 shows the critical wind speeds of vehicle models for all true wind directions. The lowest critical wind speed appeared near a wind direction of 45 ° except for the coach. As for the coach,

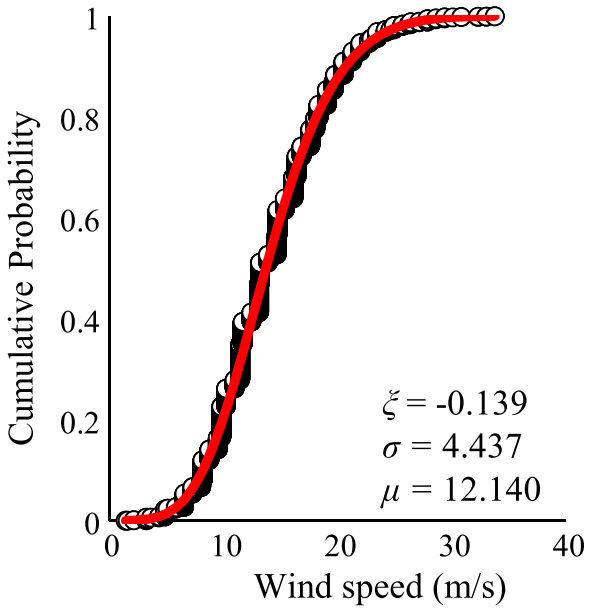

Fig. 11. Estimated cumulative distribution function for NW direction.

the lowest critical wind speed for a sideslip accident was obtained at a wind direction of 110 °, which corresponded to an effective wind direction of 90 °. Since the effective wind direction is based on vehicle speed as well as the true wind speed vector, the lowest critical wind speed is subject to variation by several factors.

As shown in Fig. 14, an overturning accident was governed by the critical wind speed in most wind directions for the large van, the tractor-trailer, and the truck. In the case of the coach, both types of accidents were anticipated according to wind direction. However, only a sideslip accident was predicted for the passenger car.

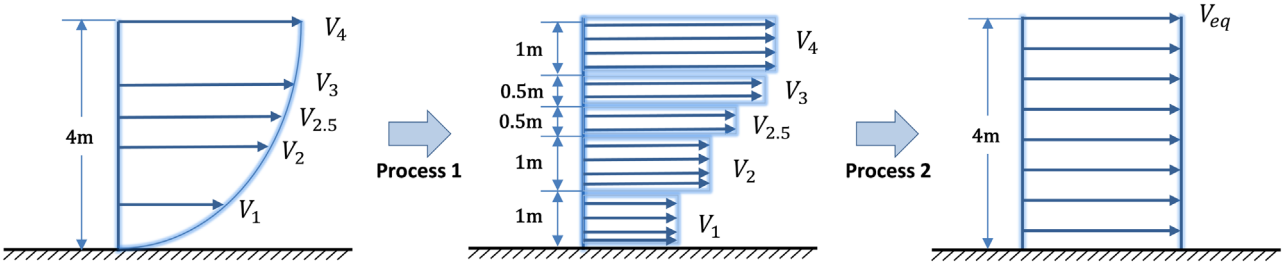

Fig. 10. Procedure to calculate equivalent wind speeds.

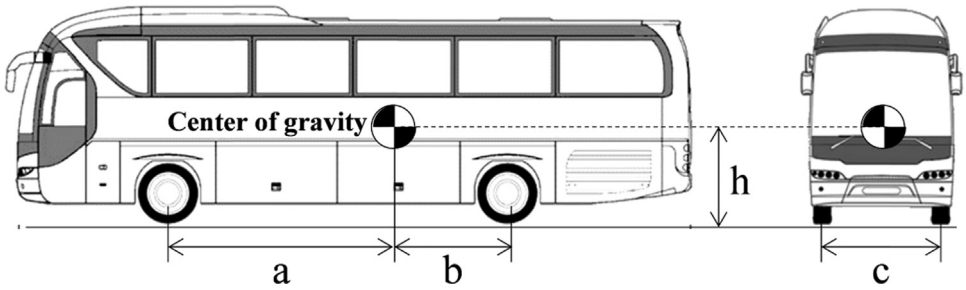

Fig. 12. Dimensions and center of gravity of a coach.

Table 2
Dimensions of investigated vehicles.

	Passenger car	Coach	Large van	Tractor-trailer	Truck
Mass (kg)	1500	7500	6000	10,000	13,700
a (m)	1.0	4.0	4.0	3.0	4.6
b (m)	1.5	2.0	2.0	6.0	6.4
c (m)	1.5	2.0	2.0	2.0	2.55
h (m)	0.5	1.0	1.0	1.5	1.5
Frontal Area (m^2)	2.5	8.0	10.0	10.0	10.2

4. Case study for vulnerability assessment

The annual number of days for traffic control, N_C, could be estimated for the examined bridge based on critical wind-speed direction graphs. Fig. 15 shows the estimated N_C for each traffic lane and vehicle model. The lane numbers are assigned from the NW to the SE direction. It is assumed that traffic keeps to the right lanes on the bridge, which means that lanes 1, 2, and 3 are southbound while lanes 4, 5, and 6 are northbound. For more in-depth investigation, critical factors such as the vehicle type, the position of the loading lane, the bridge direction, and the vehicle speed were examined to determine how much influence these had on the N_C.

4.1. Vehicle type

According to Fig. 15, there are significant differences in the estimated N_C between vehicle types. Vehicle types were divided into two groups depending on these results.

The first group consisted of cars, coaches and trucks, which had a value for N_C that was lower than 2 days. Large vans and tractor-trailers composed a second group that had a much higher value for the N_C.

The main difference between the two groups was the variations in aerodynamic forces and moments according to the vehicle shape. According to Eqs. (9) and (10), the aerodynamic forces and moments acting on a vehicle are highly dependent on aerodynamic coefficients and on the frontal area of the vehicle. The influence of the two factors can be seen in a comparison between the results of the coach and the large van. Although both vehicles had the same length and the same height for the center of gravity, the estimated N_C for the large van was almost twenty-four times that of the coach. The big difference originated from the fact that the aerodynamic coefficient of the rolling moment for the van was 1.6 times larger than that for the coach. The frontal area of the van was also 1.25 times that of the coach.

Vehicle weight was another of the influential factors. In order to estimate the influence of this parameter on N_C, the loading weight of the tractor-trailer was increased in intervals of 25%, and was then tested on lane 1. As shown in Fig. 16, the N_C decreased exponentially as loading weight increased. The N_C reached 16.57 days for an empty tractor-trailer, while it was reduced to one-sixth as the vehicle was loaded to 50% of its weight. When a vehicle was loaded to 100% of its weight, the N_C fell to lower than 1.0.

4.2. Loading lane

Two tendencies can be identified in Fig. 15 regarding the loading lane of a running vehicle. The first was a decrease in N_C as the loading lane moved to the inside on the bridge deck. This tendency was closely related to the position-dependency of the modification factor demonstrated in Section 3.2. Since the wind velocity distribution over the deck can be greatly affected by the shapes of girders, as well as by details such as railings, the position of a running vehicle is also a critical factor in safety assessment.

The other tendency was that the N_C for lanes 1, 2 and 3 were larger than those for lanes 4, 5 and 6. This difference originated

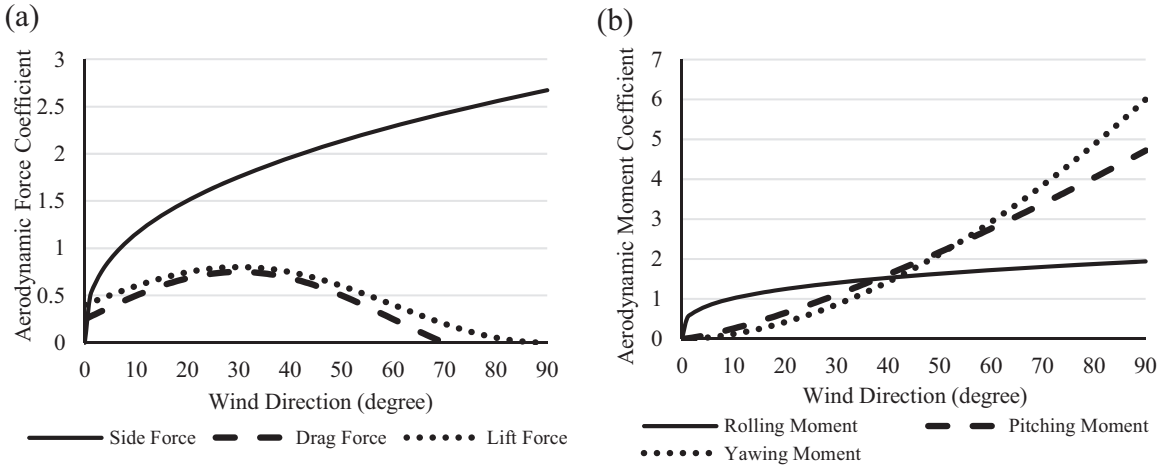

Fig. 13. Aerodynamic coefficients of a coach ($0° \le \psi \le 90°$). (a) Aerodynamic force coefficients and (b) Aerodynamic moment coefficients.

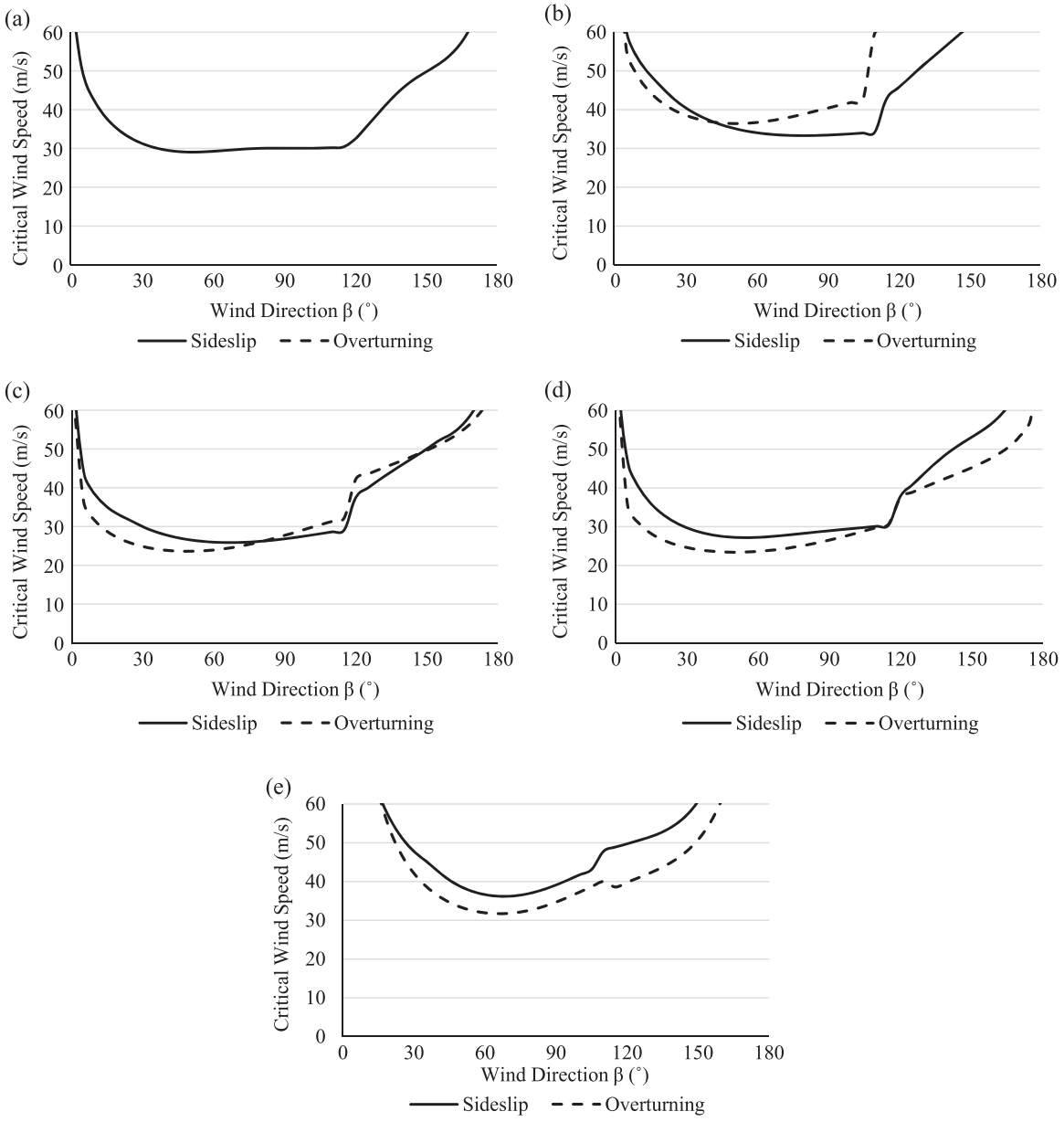

Fig. 14. Critical wind speed/wind direction graph (vehicle speed = 50 km/h) for (a) Car, (b) Coach, (c) Large Van, (d) Tractor-Trailer and (e) Truck.

from an imbalance in the distribution of the wind data across the 16 directions. The ratio of a high wind speed is direction-dependent. The west and south winds, which were the most unfavorable for vehicles running on lanes 1, 2 and 3, the frequencies of the high wind speeds over 15 m/s were 19.1 and 21.8%, respectively, whereas those for the east and north winds were only 4 and 10%, respectively. As shown by Fig. 7, the NW, NWN and NNW winds were an absolute majority (50%) of the observed wind data, and this biased distribution of wind data led to disproportionate results for the N_C between the two groups of loading lanes.

4.3. Bridge direction

As described in Section 4.2, the dominant wind direction significantly affected the vulnerability of running vehicles. The bridge direction, which is determined in the early stages of bridge planning, can also affect this vulnerability. In order to investigate this affect, the longitudinal direction of the bridge was artificially rotated from its northeast-southwest to a north-south direction by 45 ° in a counterclockwise direction. The values for N_C for the rotated bridge were quite different from those for the original bridge, as shown in Fig. 17. The values for N_C for lanes 1, 2 and 3 were greatly reduced whereas those for lanes 4, 5 and 6 were not. This change was brought about by the change in the critical wind speed for each wind direction according to the rotation of the bridge direction. Almost half of the estimated N_C for lanes 1, 2 and 3 were induced by the impact of the WNW and NW winds on the original bridge location. By rotating the bridge direction, however, the critical wind speeds for the vehicles on the lanes 1, 2 and 3 were increased due to the obtuse angle between the dominant wind direction and the vehicle direction, and this change led to a great decrease in the estimated N_C for these wind directions. On the other hand, a running vehicle on lanes 4, 5 and 6 had angles of 45 ° and 67.5 ° from WNW and NW winds, which can be categorized as dangerous angles in terms of vehicle safety, as shown in Fig. 14. Accordingly, the dominant wind directions

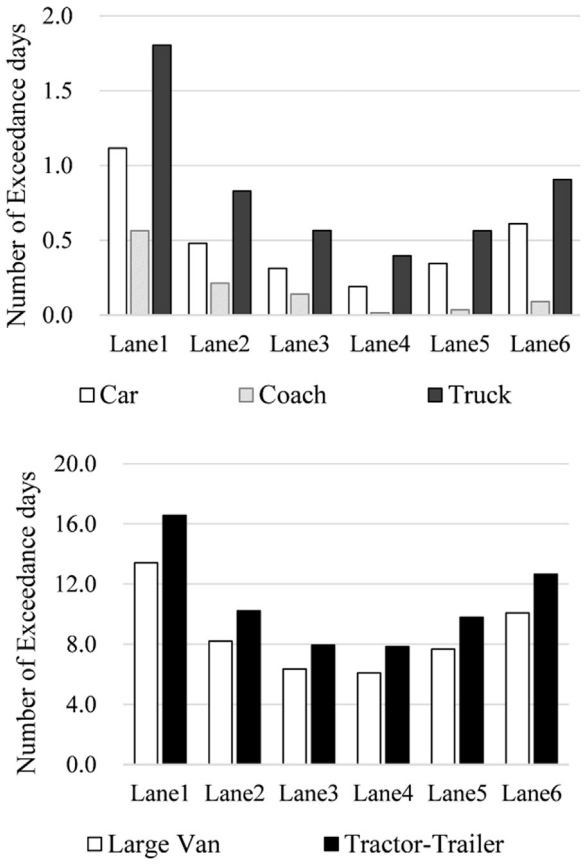

Fig. 15. N_C of all vehicle models for 6 lanes.

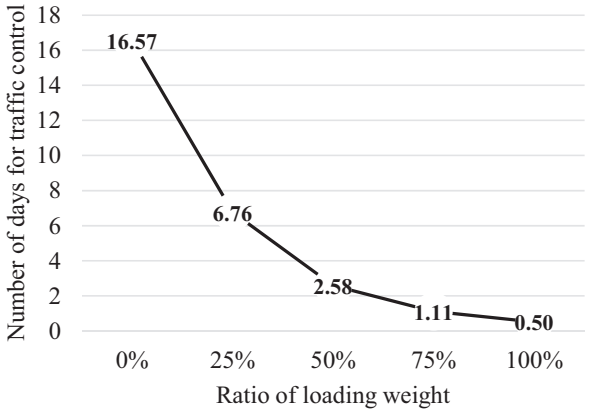

Fig. 16. N_C of the tractor-trailer according to the ratio of loading weight on lane 1.

increased the estimated N_C while that for other wind directions somewhat compensated with a decrease. This considerable change in the estimated N_C indicates the importance of bridge alignment on vehicle safety is relative to the dominant wind direction for a given bridge site.

4.4. Vehicle speed

In order to examine the effect of the vehicle speed on the N_C, the vehicle speed was varied from 10 to 110 km/h at intervals of 10 km/h. Fig. 18 shows the variation in N_C for a tractor-trailer running on lane 1. The N_C increased exponentially as vehicle speed increased. The N_C remained at a low level until the vehicle speed reached 50 km/h, but it started to increase dramatically when the vehicle speed exceeded 50 km/h. Reducing the vehicle speed from

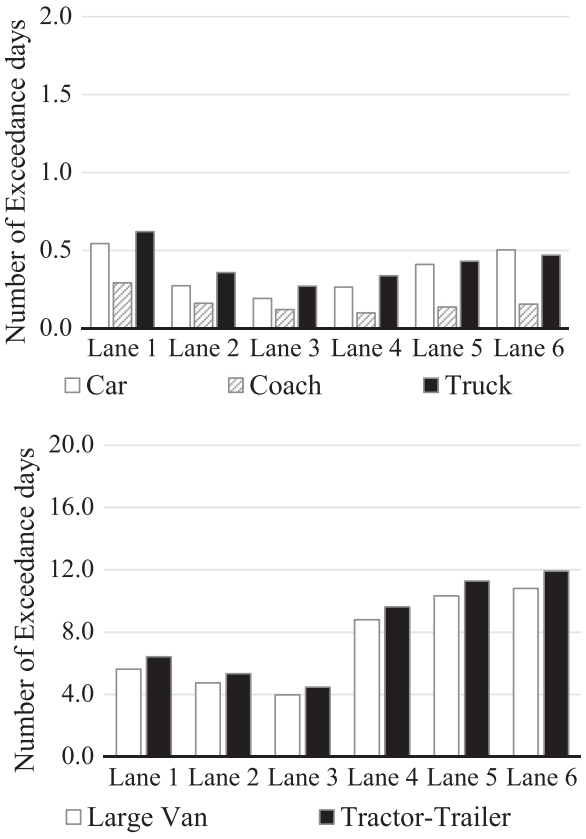

Fig. 17. N_C of all vehicles for a rotated bridge.

100 to 50 km/h resulted in an approximately 80% reduction in the N_C. This considerable change demonstrates the critical influence that vehicle speed exerts on crosswind hazards. The control of speed limits can be a highly effective and efficient measure in securing vehicle safety in predictably strong wind conditions.

5. Conclusions

This paper proposes a method to assess the frequency of the exposure to hazardous crosswinds by estimating the value for N_C. The assessment was proceeded by considering the effect that 16 different wind directions could exert on various types of vehicles. The method was applied to an example bridge for five different vehicle types. In order to estimate the N_C for each traffic lane, wind tunnel tests to measure the increasing effect of wind speed over the bridge deck were performed. Based on the assessment results, the following conclusions were drawn:

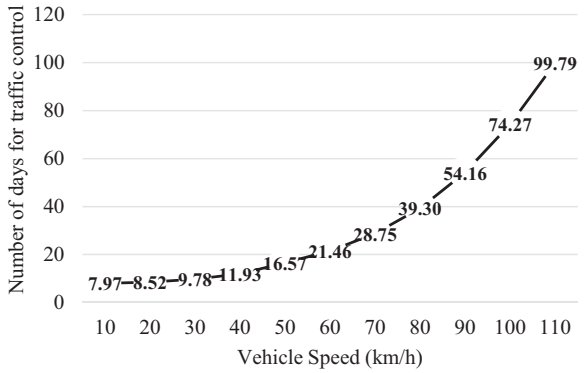

Fig. 18. N_C of the tractor-trailer according to vehicle speed on lane 1.

(1) The vehicle shape and dimensions has a great impact on the assessment results. A more than 10-fold difference was observed among the vehicle types considered. Weight was an influential factor in determining the N_C for a tractor-trailer.
(2) Bluff girders affected the wind flow over the deck. Wind speeds varied among the traffic lanes, and along the height above the road surface. These variations resulted in differences in the estimated N_C among traffic lanes. Variations in N_C were similar to the variations in factors that increased wind speeds for each lane. This showed that girder shape and the arrangement of traffic lanes are among the factors influencing vehicle vulnerability to crosswinds.
(3) Vehicle speed is also an influential factor on vehicle vulnerability to crosswinds. A dramatic decrease in N_C is expected when vehicle speed is reduced by half for a tractor-trailer running on the windward lane. Consequently, a reduction in the speed limit to a proper level can be an effective and efficient measure in securing the safety of high-sided vehicles in crosswinds.
(4) The relative angle between the dominant wind direction and a bridge layout critically affects the vehicle vulnerability to crosswinds. Since the speed of a running vehicle is also incorporated with this relative angle in the assessment of vehicle vulnerability, such a consideration should be one of the major issues in the planning stages of sea-crossing bridges that are subject to frequent crosswinds.

Acknowledgments

The authors gratefully acknowledge financial support (Project no. 0583-20130036) from Hyundai Engineering and Construction through the Institute of Construction and Environmental Engineering at Seoul National University. Also, this research was supported by a grant (09CCTI-A052531-05-000000) from the Ministry of Land, Transport and Maritime Affairs of the Korean government through the Core Research Institute at Seoul National University for Core Engineering Technology Development of Super Long Span Bridge R&D Center.

References

Baker, C.J., 1986. A simplified analysis of various types of wind-induced road vehicle accidents. J. Wind Eng. Ind. Aerodyn. 22, 69–85.
Baker, C.J., 1987. Measures to control vehicle movement at exposed sites during windy periods. J. Wind Eng. Ind. Aerodyn. 25, 151–161.
Baker, C.J., 1991a. Ground vehicles in high cross winds. 1. Steady aerodynamic forces. J. Fluids Struct. 5, 69–90.
Baker, C.J., 1991b. Ground vehicles in high cross winds. 2. Unsteady aerodynamic forces. J. Fluids Struct. 5, 91–111.
Baker, C.J., 1991c. Ground vehicles in high cross wind. 3. The interaction of aerodynamic forces and the vehicle system. J. Fluids Struct. 5, 221–241.
Baker, C.J., Reynolds, S., 1992. Wind induced accidents of road vehicles. Accid. Anal. Prev. 24 (6), 559–575.
Baker, C.J., 2015. Risk analysis of pedestrian and vehicle safety in windy environments. J. Wind Eng. Ind. Aerodyn. 147, 283–290.
Batista, M., Perkovič, M., 2014. A simple static analysis of moving road vehicle under crosswind. J. Wind Eng. Ind. Aerodyn. 128, 105–113.
Chen, S.R., Cai, C.S., 2004. Accident assessment of vehicles on long-span bridges in windy environments. J. Wind Eng. Ind. Aerodyn. 92, 991–1024.
Coles, S., 2001. An Introduction to Statistical Modeling of Extreme Values. Springer, London.
Kim, D.H., Kwon, S.D., Lee, I.K., Jo, B.W., 2011. Design criteria of wind barriers for traffic. Part 2: decision making process. Wind Struct. 14, 71–80.
Korean Society of Civil Engineers, 2006. Design Guidelines for Steel Cable-Supported Bridges, Korea.
Kwon, S.D., Jeong, U.Y., 2005. An overall wind shielding program for enhancing driving stability. J. Korean Soc. Steel Constr. 17 (3), 263–270.
Kwon, S.D., Kim, D.H., Lee, S.H., Song, H.S., 2011. Design criteria of wind barriers for traffic. Part 1: wind barrier performance. Wind. Struct. 14, 55–70.
Xu, Y.L., Guo, W.H., 2003. Dynamic analysis of coupled road vehicle and cable-stayed bridge systems under turbulent wind. Eng. Struct. 25, 473–486.
Zhu, L.D., Li, L., Xu, Y.L., Zhu, Q., 2012. Wind tunnel investigations of aerodynamic coefficients of road vehicles on bridge deck. J. Fluids Struct. 30, 35–50.